Flame pyrolysis – a preparation route for ultrafine pure γ-Fe_2O_3 powders and the control of their particle size and properties

S. GRIMM, M. SCHULTZ, S. BARTH*
Friedrich Schiller University, Institut für Anorganische und Analytische Chemie, August-Bebel-Str. 2, D-07743 Jena, Germany

R. MÜLLER
Institut für Physikalische Hochtechnologie, Helmholtzweg 2, D-07743 Jena, Germany

Highly dispersed γ-Fe_2O_3 powders with particle sizes down to 5 nm were directly synthesized by combustion of solutions of iron pentacarbonyl or iron(III) acetylacetonate in toluene in an oxyhydrogen flame. The particle size as well as other properties of the obtained powders can be controlled simply by varying the iron concentration in the starting solutions. Phase composition, morphological and magnetic properties of the powders were studied. The reasons for the formation of γ-Fe_2O_3 are discussed by means of structure–chemical/kinetic considerations. The materials are interesting as recording materials, or ferrofluids, or for colour imaging and bioprocessing.

1. Introduction

Systematic investigations of phase and particle formation under extreme conditions in an oxyhydrogen flame [1] for preparation of nanosized powders with extraordinary properties have focused our attention on γ-Fe_2O_3, which is widely used for recording materials, magnetic fluids and colour pigments. While conventional preparation routes for γ-Fe_2O_3 are rather complex, usually including many steps, efforts have been made to establish direct preparation methods [2, 3].

For this purpose, gas phase reactions and the pyrolysis of highly dispersed droplets of solutions of iron(III) compounds seem to be the most promising approaches to prepare nanoscaled iron oxides.

Generally, the two main preparation routes employed are:

(a) spray pyrolysis process in a classical sense, based on the thermal decomposition of an aerosol of metal salt solutions at relatively low temperatures (usually 500–1000 °C); and
(b) more complex methods typically containing a condensation process from the gas phase for the particle formation.

1.1. Spray pyrolysis

The formation of iron oxide particles by spray pyrolysis of iron compounds dissolved in organic solvents or water in combination with further thermal treatment of the obtained powders is reported by several authors.

Kato and Tokunaga [4] described the spray pyrolysis of an iron(III) nitrate solution at temperatures of 700–1000 °C. A mixture of different iron oxides such as FeO, γ-Fe_2O_3 and Fe_3O_4 always resulted, with mean particle sizes of about 1 μm.

In contrast, Kagawa *et al.* [5] prepared much smaller iron oxide particles of about 10 nm, also starting from iron(III) nitrate solutions by spraying the mist in an inductively coupled plasma at extremely high temperatures obtaining γ-Fe_2O_3 as the main phase together with traces of α-Fe_2O_3 and iron oxohydroxides.

Recently, Gonzàlez-Carreño *et al.* [6], Cabanas *et al.* [7] and Morales *et al.* [8] carried out more detailed investigations of the synthesis of various iron oxide phases by means of spray pyrolysis. They used starting materials such as $Fe(NO_3)_3 \cdot 9H_2O$, $FeCl_3 \cdot 6H_2O$, iron(III) citrate and ammonium iron(II) citrate [6, 7], varied the solution concentration and the streaming velocity of the carrier gas and obtained iron oxide powders of different morphologies, phase compositions and magnetic properties. They found that only quite distinct starting compounds and reaction conditions lead to γ-Fe_2O_3, frequently containing various amounts of hydroxide phases and α-Fe_2O_3 impurities.

* Author to whom correspondence should be addressed.

0022–2461

1.2. Gas phase reactions

As early as 1926, Wedekind and Albrecht [9] prepared iron oxides for pigments and polishing materials by the controlled combustion of $Fe(CO)_5$. They observed the formation of reddish powders, containing α-Fe_2O_3 and γ-Fe_2O_3 as major phases. Kohlschütter and Tüscher [10] used another gas-phase reaction for the synthesis of iron oxides, namely the reaction between metallic iron and carbon electrodes in a light arc. Cagliotti and D'Agostino [11] identified the resulting powder as ferrimagnetic γ-Fe_2O_3. (Later it was postulated by Haul and Schoon [12] that really pure γ-Fe_2O_3 is only obtained in a light arc under oxidizing conditions.) Winkel and Haul [13] systematically studied the formation of γ-Fe_2O_3 by the combustion of $Fe(CO)_5$ aerosols in relation to the particle size and crystallinity of the resulting powders. In 1949, the synthesis of black, very fine and uniform magnetic Fe_3O_4 by the combustion of liquid $Fe(CO)_5$ in compressed air at temperatures between 1400 and 1500 °C was reported in a BASF patent [14].

A very important example for the technical application of gas-phase reactions is the so-called Aerosil process, used for the preparation of nanoscaled, highly dispersed powders such as SiO_2, TiO_2, Al_2O_3, ZrO_2 and several iron oxides. The high temperature hydrolysis of $SiCl_4$ in an oxyhydrogen flame for the preparation of highly dispersed silica powders was first introduced by Klöpfer in 1942 [15]. Later this method was extended to many other volatile metal chlorides to get a variety of nanosized, so-called "fumed oxides" [16]. The combustion of metal chlorides for powder preparation has, however, a few disadvantages [17]:

1. The powders are usually contaminated with chloride ions, a fact, which makes these materials unsuitable for direct use in ceramics.
2. In most cases, further treatment is necessary to remove the impurities. Unfortunately, washing or thermal treatment leads to a loss of the unique morphological properties.
3. It is very difficult to prepare binary or even more complex oxide compounds, such as doped zirconia, spinels, perovskites, phosphates etc., using a direct route.
4. The structure-directing influence of the chloride ions leads, in the case of iron chloride, to the formation of β-Fe_2O_3 [18, 19].

In a previous publication [20], we described the formation of such oxides by the combustion of complex metal compounds as acetylacetonates, alkoxides, ethylhexonates or metal organic compounds in a turbulent oxyhydrogen flame.

The use of such raw materials, free of undesirable elements such as chlorine, sulfur or nitrogen, is an important prerequisite to avoid the formation of secondary phases as chlorides or sulfates in the final products of the combustion process.

From the literature it appears that the formation of iron oxide phases in a spray pyrolysis process or by gas phase reactions differs in the resulting end products. Therefore it was interesting to carry out the iron oxide formation in an oxyhydrogen flame, starting from quite different materials, to study its influence on the particle size and the magnetic properties of the resulting powders. Thus, the synthesis of γ-Fe_2O_3 from $Fe(CO)_5$ and iron(III) acetylacetonate in such a flame pyrolysis process is reported below.

2. Experimental procedure

Different amount of $Fe(CO)_5$ and iron(III) acetylacetonate were dissolved in toluene and burned under identical conditions in an oxyhydrogen flame ($T > 2500$ K, 5 ml solution/min, $pO_2 = 0.4$ MPa, $pH_2 = 0.11$ MPa) as described in [1]. A schematic diagram of the experimental flame reactor is given in Fig. 1. The fumed powders were collected with the help of an electrostatic filter (voltage 6 kV, 5 mm electrode distance) and the yield was always about 90%. The properties of the powders were investigated with the following methods:

- nitrogen sorption measurements at 77 K after evacuating the samples at 523 K using an automated sorptometer; the specific surface area (S_{BET}) was determined by the multi-point Brunauer–Emmett–Teller (BET) method, the pore volume from the "Gurvich" rule and the nature of the pores by means of the *t*-plot and the Pierce method.
- infrared spectroscopy; KBr technique, IR 2000 (Perkin Elmer).
- dynamic light scattering for the determination of the particle size in water at pH = 3; solid content 100 mg dm^{-3}, using the Stokes–Einstein relation, ELS 800 (Otsuka Electronics).
- X-ray powder diffraction for the determination of the phase composition and the primary crystal size; MoK_α or CuK_α radiation, HZG 4 (Freiberger-Präzisionsgeräte)
- transmission electron microscopy (TEM; Tesla Inc.)
- measurements of the specific saturation magnetization (σ_∞, values extrapolated to $H \to \infty$), relative saturation remanence ($m_r = M_r/M_\infty$) and of the coercivity (H_c) by means of a PAR (Princetown Applied Research) vibrating sample magnetometer ($H_{max} = 1200$ kA m^{-1}).

3. Results and discussion

An overview of the solution concentrations and the most important properties of the obtained powders is given in Table I.

3.1. Powders prepared from an iron(III) acetylacetonate solution

The combustion of a 0.3 M solution of iron(III) acetylacetonate in toluene yielded a red–brown, ferrimagnetic powder. The mean particle size, calculated from the value of the specific surface area ($S_{BET} = 133$ m^2 g^{-1}) is about 9 nm. A transmission electron micrograph of the powder is shown in Fig. 2a. The particles have a spherical shape, comparable with powders prepared by spray pyrolysis, but in contrast to the latter their size is much smaller because of

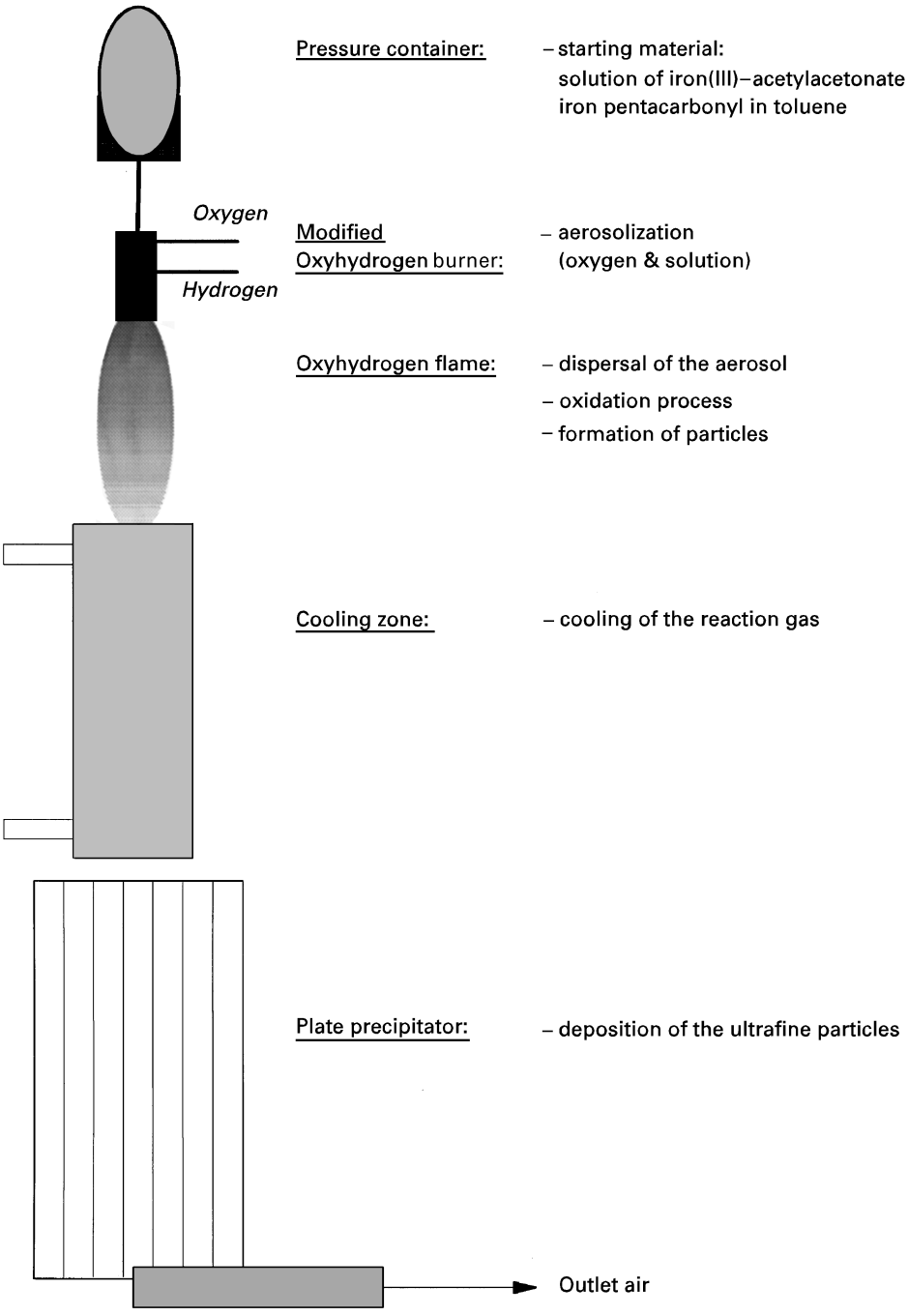

Figure 1 Schematic diagram of the experimental flame reactor.

a lower degree of aggregation, i.e. the observed objects are really the primary particles. Despite their very small size they agglomerate weakly. Their dimensions on the micrographs agree well with the mean particle sizes based on BET data. The spherical shape can be caused either by the fact that the particles passed a liquid phase as droplets and became solid in the cooler parts of the flame after burning, comparable with the formation of a hailstone, or by a condensation process from the vapour phase, like the formation of a snowflake.

In case of the condensation mechanism the resulting powder should be characterized by a higher percentage of intraparticular voids in relation to powders, which have passed a liquid phase. That is why the estimation of the pore size distribution on the basis of sorption measurements is a useful tool to make a determination between the occurring mechanism. A more detailed description is given in Section 3.3. The X-ray diffraction pattern as well as the i.r. spectra clearly indicate the existence of γ-Fe_2O_3 in the obtained powders. The powder patterns are distinctly broadened, caused by the small grain size. To explain the difference between the values of the mean particle size based on the multi-point BET data (9 nm) and on the line broadening of the X-ray pattern with the Scherrer formula (6 nm), it should be kept in mind that in the case of X-ray diffraction the average grain sizes of the samples are considered, whereas the BET-data and TEM reflects the morphology, i.e. the particle size.

Gonzáles-Carreño *et al.* [6], obtaining monodispersed nanoparticles of a size of 5 nm by spray pyrolysis

TABLE I Properties of the γ-Fe_2O_3 powders

	FPACAC	FPCO1	FPCO2	FPCO3
Starting solution				
iron compound	$Fe(acac)_3$	$Fe(CO)_5$	$Fe(CO)_5$	$Fe(CO)_5$
iron concentration (mol dm^{-3})	0.3	0.5	1.8	3.6
Physical properties				
S_{BET} (m^2 g^{-1})	133	103	85	66
S_T (m^2 g^{-1})	135	102	83	75
d_{BET} (nm)	9	12	14	19
d_{XRD} (nm)	6	6	21	28
d_{ELS} (nm)	30 ± 15	29 ± 15	32 ± 15	45 ± 20
pore volume (cm^3 g^{-1})	0.35	0.25	0.20	0.20
Magnetic properties				
σ_∞ (e.m.u g^{-1})	36.6	32.9	52.8	62.8
σ_{15} [$H = 15$ kOe] (e.m.u g^{-1})	35.5	31.3	51.5	62.1
remanence M_r/M_∞	0.02	0.04	0.12	0.17
coercivity H_c (Oe)	6	18	52	80
coercivity H_c (kA m^{-1})	0.5	1.4	4.1	6.4
Thermal properties (DSC onset)				
exothermic I A (°C)	150	150	140	–
exothermic I B (°C)	230	245	210	230
exothermic II (°C)	500	460	500	515

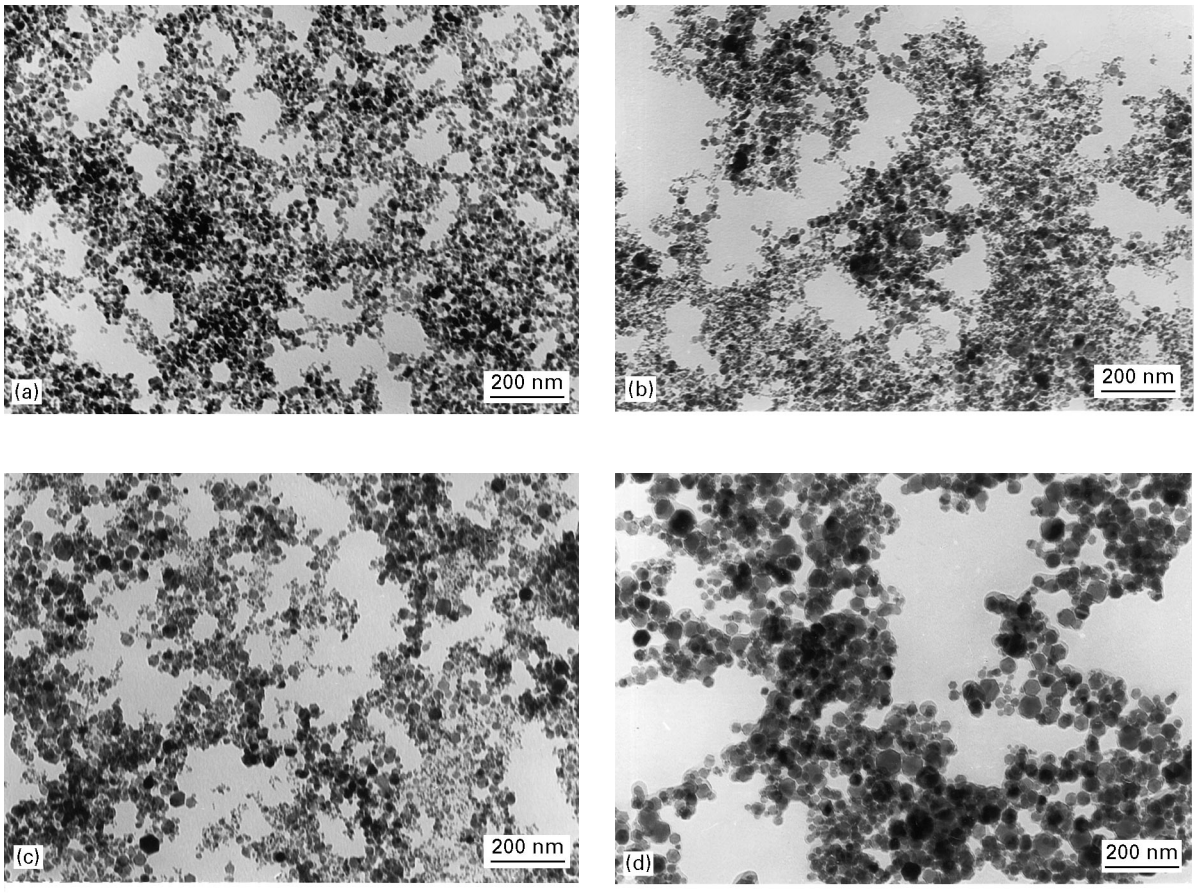

Figure 2 Electronmicrographs of ultrafine γ-Fe_2O_3-powders prepared by flame pyrolysis: (a) FPACAC starting from a 0.3 M solution of iron(III) acetylacetonate in toluene. (b) FPCO1 starting from a 0.5 M solution of $Fe(CO)_5$ in toluene. (c) FPCO2 starting from a 1.8 M solution of $Fe(CO)_5$ in toluene. (d) FPCO3 starting from a 3.6 M solution of $Fe(CO)_5$ in toluene.

of iron(III) acetylacetonate dissolved in ethanol, discussed the particle size in terms of an exothermic oxidation reaction (decomposition) of the particle aggregates, whose shape and size result from the preliminary aerosol droplets. The formation of pure γ-Fe_2O_3 is in contrast to the results of Kagawa *et al.* [5], who prepared iron oxide powders by the spray pyrolysis of ferric nitrate solutions in an inductively coupled

plasma at extremely high temperatures. By this method they observed α-Fe_2O_3 as well as γ-Fe_2O_3, discussing the formation of the latter as a low temperature process below 550 °C.

Hence, structure and size of the resulting iron oxide particles are strongly influenced by the nature of the starting solution, the droplet size, the temperature and the retention time during the process. Conventional spray pyrolysis should yield bigger particles which are aggregates of smaller primary particles with narrower size distribution. The size of these aggregates or agglomerates can be calculated from the size of the droplets, the concentration of the solution and the molar weight of the raw materials, keeping the volume of pore space in mind [21]. The structure of the resulting iron oxide phase is however predominately determined by the nature of the starting solution and by the temperature and retention time during the process.

A decomposition–condensation mechanism should be considered, involving a breakage of the FeO–C bonds followed by a condensation step leading to the iron oxide structure. This hypothesis was first proposed by Winkel and Haul in 1938 [13], studying systematically the oxidation of iron pentacarbonyl in a preheated quartz tube under different oxygen partial pressure. At oxygen concentrations below 0.1% a complex mixture of metallic iron and unspecified iron oxide particles was observed, explained by the formation of an aerosol of metallic iron which was partially oxidized to γ-Fe_2O_3 in a succeeding process. The formation of α-Fe_2O_3 is prevented by a short retention time. At 2% oxygen and 900 °C pure γ-Fe_2O_3 was formed, whereas the oxidation with pure oxygen yielded an amorphous iron oxide.

Higher oxygen pressure apparently suppressed the formation of an aerosol of metallic iron. Since the tendency for the crystallization of iron oxide is significantly less than that for elemental iron only amorphous iron oxide was formed.

Schrader and Büttner [22] studied the pickle (burn off) of iron electrodes in an electrical arc in an oxygen flow. They reported always obtaining a mixture of different oxide phases with γ-Fe_2O_3 as major phase accompanied by α-Fe_2O_3 and ε-Fe_2O_3. This experiment was a strong clue as to the stability of γ-Fe_2O_3 at elevated temperatures, even if there is no further stabilization of this phase by impurity traces such as Fe^{2+}, alkali ions, carbon or water.

3.2. Powders prepared from iron pentacarbonyl solutions

Because of the quite different findings in the literature about phase formation during different combustion processes we had also burned iron pentacarbonyl in an oxyhydrogen flame in order to determine if the formation of γ-Fe_2O_3 was predominately due to the conditions in the flame or due to the nature and the properties of the starting materials.

For a comparison with the properties of the powders prepared from iron(III) acetylacetonate, it was important to establish a similar iron concentration ($\sim$0.5 M Fe) in the starting solution, limited by the solubility of iron(III) acetylacetonate in toluene. The direct combustion of iron pentacarbonyl in air was already investigated many years ago [14] leading to the formation of very fine black Fe_3O_4. To understand this behaviour the conditions in such a flame must be considered. As in the flame of a candle, in which a spontaneous combustion without sufficient oxygen forms soot, so too, the burning of iron pentacarbonyl in a free flame forms Fe_3O_4 because of the lack of oxygen.

Surprisingly, the combustion of a 0.5 M $Fe(CO)_5$ solution in an oxyhydrogen flame, in contrast to the spontaneous combustion in air, resulted in the formation of single-phase γ-Fe_2O_3, as well. An example is shown in Fig. 3 (sample FPCO3, measured with MoK_α radiation) and compared with data from the JCPDS-ICDD-powder diffraction data system (File 39-1346).

The properties of the obtained red–brown powder (FPCO1 in Table I) agree well with those of the powders from iron(III) acetylacetonate. The specific surface area, $S_{BET} = 103\ m^2\ g^{-1}$, provides an average particle size of 12 nm. The transmission electron micrograph shown in Fig. 2b is very similar to that of FPACAC (Fig. 2a), showing weakly agglomerated, spherical primary particles. Hence, the same particle formation mechanism is likely, regardless of the very different starting materials. The Winkel and Haul mechanism seems to be convincing, but it cannot simply be extended to our experiments. Possibly, the iron aerosol can, but does not necessarily need to act as precursor for the formation of γ-Fe_2O_3 in the flame.

In fact, the formation of such an iron aerosol in an oxyhydrogen flame is rather unlikely, despite the zero oxidation state of iron in iron pentacarbonyl. In the case of iron(III)-acetylacetonate, which also yields γ-Fe_2O_3, the probability of the necessary reduction of Fe^{3+} to Fe^0 in a first step followed again by an oxidation is, because of the very short retention time in the flame, very low. There should be a specific correlation between the particle size of the fumed powders and the iron concentration in the starting solutions.

Hence, we have studied the high temperature combustion of higher concentrated $Fe(CO)_5$ solutions (1.8 and 3.6 M). The results are summarized in Table I (FPCO2 and FPCO3), and the corresponding transmission electron micrographs are given in Fig. 2c and d. It is clearly seen that a more highly concentrated starting solution results in a significant increase of the particle size.

The relationship between iron concentration and particle size based on the BET data is illustrated in Fig. 4. The slope of the curve in the investigated concentration range is almost linear. Two more facts have to be kept in mind: (i) the particle size is a mean value; and (ii) the bigger the particles the broader is the particle size distribution. There is a sharp lower limit of the distribution at 5 nm, which is the lower processing limit of the electrostatic filter used for the powder collection. The particle size distribution is

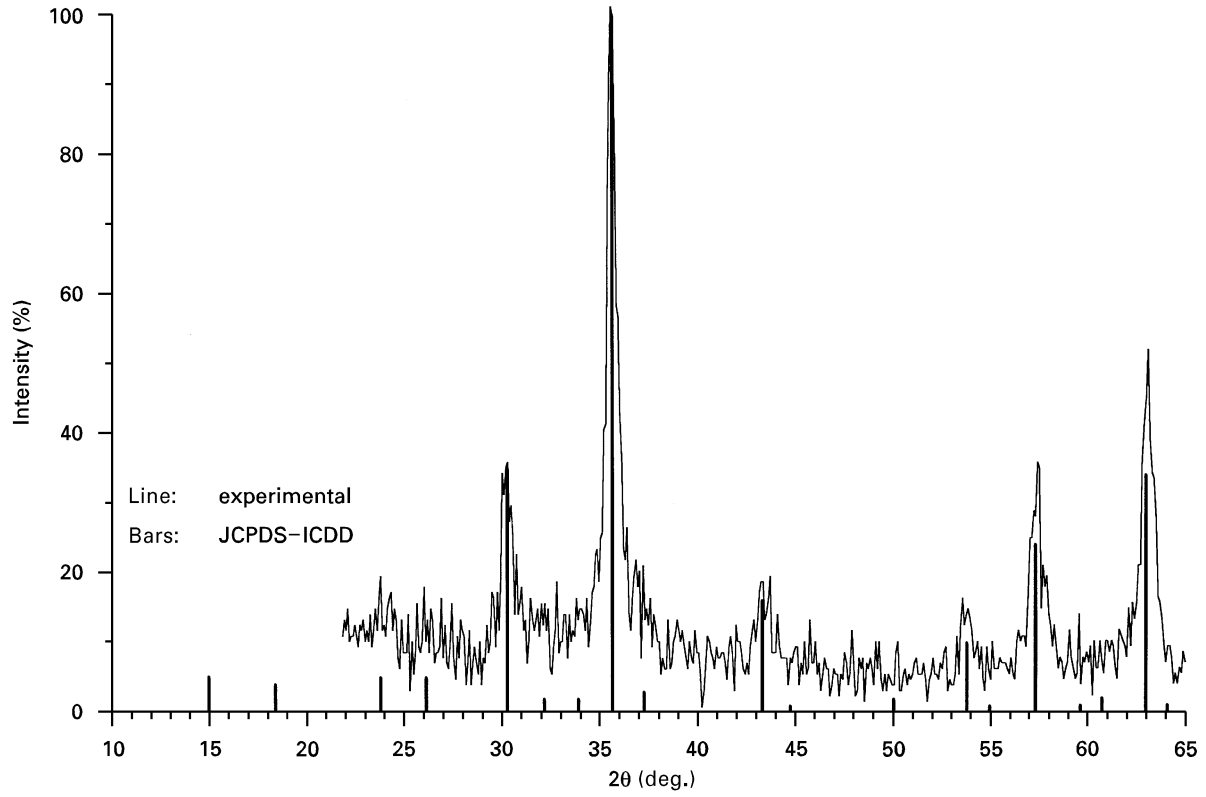

Figure 3 The X-ray diffraction pattern of powder FPCO3 (lines), compared with data for pure γ-Fe_2O_3 from literature (JCPDS powder diffraction file 39-1346, bars).

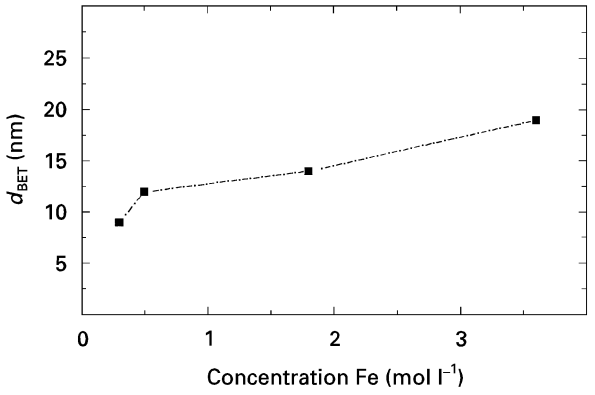

Figure 4 Relationship between the particle size of the prepared γ-Fe_2O_3-powders derived from BET data (d_{BET}) and the iron concentration of the starting solutions.

a possible clue to the particle formation mechanism in the flame.

3.3. Physisorption measurements

In Fig. 5 the adsorption-desorption isotherms together with the *t*-plot of the four powders under investigation are given. The isotherms are always qualitatively similar, they can be interpreted according to the Brunauer classification as a combination of type IV and type II.

The estimated differences in the amount of adsorped nitrogen arise from the different particle sizes and different interparticular voids of the powders. It is striking that in all cases no significant hysteresis between adsorption and desorption is detectable, an indication that adsorption and desorption proceed in the same manner.

Moreover it can be derived from the shape of the isotherms that multilayer adsorption and capillary condensation takes place simultaneously and continuously. The slope of the curves is almost continuous indicating the absence of micropores and also the complete lack of a distinguished accumulation of meso-scaled pores. Furthermore this behaviour is reflected in the *t*-plots and can be interpreted in terms of very weak aggregation forces between the primary particles. This is quite remarkable in view of the particle size and could be caused by the preparation process. As seen in the electron micrographs, the particles are nearly spherical without significant surface roughness.

The estimated values of the specific surface area derived from the *t*-plot (S_T) agree very well with the values calculated from the BET-theory (Table I).

3.4. Thermal behaviour

Differential scanning calorimetry (DSC) measurements indicate, in all samples under investigation, the presence of three exothermic effects. The values of the estimated onset-temperatures are summarized in Table I. The first DSC peak is really the combination of two simultaneous thermochemical events (labelled as "A" and "B", respectively). The first one ("A") can be attributed to the crystallization of small amounts of amorphous constituents within the ultrafine γ-Fe_2O_3-powders, having their origin in the extremely high

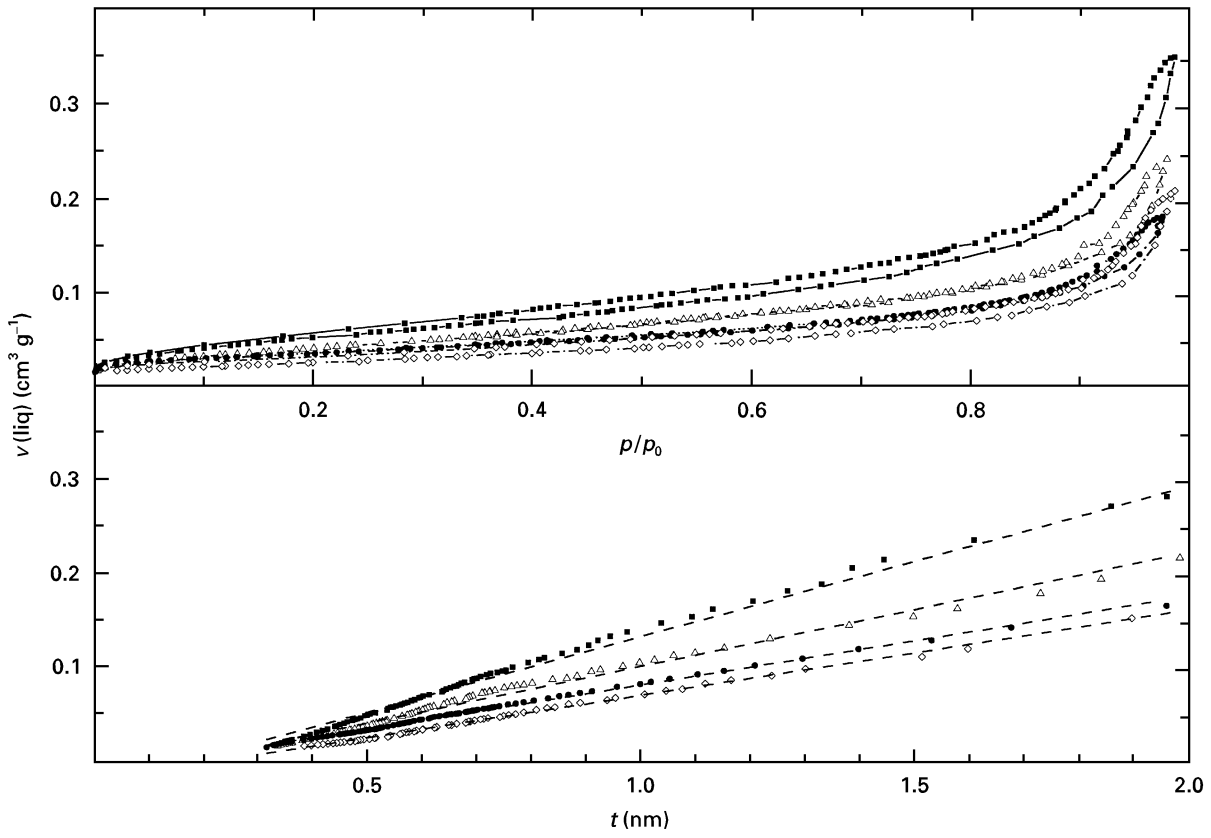

Figure 5 (a) Adsorption–desorption isotherms of the investigated γ-Fe_2O_3-powders. (b) Calculated *t*-plots and the specific surface S_T derived from the nitrogen-sorption measurements of (a). ■ FPACAC; △ FPCO1; ● FPCO2; ◇ FPCO3. S_T values ($m^2\ g^{-1}$): FPACAC, 135; FPCO1, 102; FPCO2, 83; FPCO3, 75.

cooling rates after pyrolysis. Peak "A" also occurs when the DSC measurements had been carried out under argon atmosphere, whereas peak "B" disappears. Therefore, the second event, "B", could be interpreted as the oxidation of adsorbates on the extraordinarily large surface area provided by the ultrafine powders. Accordingly both effects increase with decreasing particle sizes, i.e. with increasing specific surface area of the powders. More information about the nature of the adsorbed material is obtainable by means of i.r. spectroscopy. In Fig. 6 the i.r. spectra of the described γ-Fe_2O_3-powders are shown. First the characteristic Fe-O vibrations are detectable in the region between 400 and 900 cm^{-1}. The strong absorption band at 3400 cm^{-1} together with the band at 1620 cm^{-1} indicates the presence of adsorbed H_2O. Furthermore some broad absorption bands arise in the region between 1400–1600 cm^{-1} and 1000–1200 cm^{-1}, which are related to the vibration of a C–O-bond.

According to Hair [23] carbonate ions (CO_3^{2-}) and CO_2, which are adsorbed on the surface of a metal oxide could give rise to such an i.r. absorption between 1400–1600 cm^{-1}, but it could also result from the carboxylate groups (CO_2^-) and (HCO_2^-).

Whereas carbonate ions and adsorbed CO_2 are not oxidizable, the carboxylate groups can be readily oxidized to CO_2. Since the DSC measurements have clearly indicated the existence of oxidizable constituents within the γ-Fe_2O_3-powders, the absorption bands between 1530–1600 cm^{-1} and at 1440 cm^{-1}, respectively, cannot be attributed only to adsorbed CO_2, but rather also to the discussed carboxylate groups.

This assumption was confirmed by means of mass spectroscopy, showing a significantly higher proportion of CO^+ ions in relation to the simple desorption of CO_2 or to the decomposition of carbonates. A more detailed description of this experiment is given elsewhere [24].

The occurence of oxidizable carboxylate groups at the surface of the fumed powders could be, despite the applied excess of oxygen in the oxyhydrogen flame, explained in the following manner:

The extraordinarily high temperature favours the formation of Fe^{2+} species within the oxyhydrogen flame, this, in combination with the high cooling rate after the combustion process, leads apparently to the incorporation of Fe^{2+} into the iron oxide.

Additionally the ultrafine powders easily adsorb CO_2. Then at the active surface area an electron transfer takes place from a Fe^{2+} ion to an adsorbed CO_2 molecule in the following manner

$$[Fe^{2+}] + \{CO_2\} \rightarrow [Fe^{3+}] + \{CO_2^-\} \qquad (1)$$

giving at least the discussed carboxylate groups or, in combination with adsorbed H_2O, a formiate anion

$$2[Fe^{2+}] + \{CO_2\} + \{H_2O\} \rightarrow 2[Fe^{3+}] + \{HCO_2^-\} + \{OH^-\} \qquad (2)$$

Note, that in Equation 2 the electron transfer occurs simultaneously between four active centres at the surface. Despite the probability for the generation of

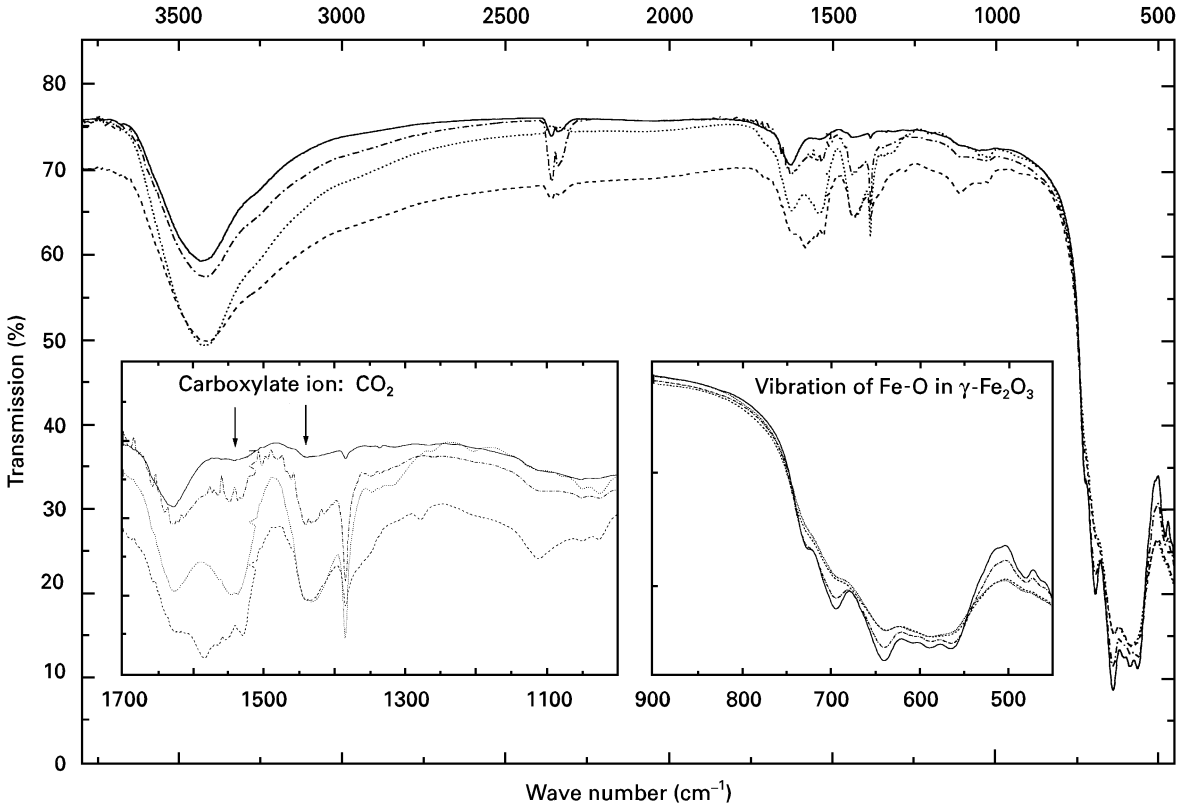

Figure 6 Infrared spectra of the described γ-Fe_2O_3 powders. —— FPCO1; –·– FPCO2; ···· FPCO3; – – – – FPACAC.

a formiate anion being very low, Equation 2 illustrates somewhat the nature of the carboxylate species; they are very reactive and oxidizable at relatively low temperatures, giving rise to the exothermic effect "B" in the DSC curve between 200 and 250 °C

$$\{CO_2^-\} + \tfrac{1}{4}O_2 \rightarrow CO_2 + \tfrac{1}{2}[O^{2-}] \qquad (3)$$

That means the adsorbed CO_2 acts as a reservoir for electrons during the oxidation process of the Fe^{2+} ions. This assumption agrees well with another experimental finding: heating the different γ-Fe_2O_3-samples under argon atmosphere (content of $O_2 < 10$ p.p.m.) always yields, in the case of powders with smaller particle sizes (e.g. sample FPACAC), black Fe_3O_4 at relatively low temperatures (250–400 °C), whereas samples with larger particle sizes (e.g. sample FPCO3) were transformed at the phase transition temperature to reddish-brown α-Fe_2O_3.

The formation of black Fe_3O_4 was not observed by heating the same samples in air. In this case all samples were transformed to α-Fe_2O_3, giving the third exothermic effect in the DSC curves (labelled as "exothermic II" in Table I). The varying reaction courses of the powders in relation to particle size can be easily explained on the basis of the discussed carboxylate species. If the particle size of the powders is greater than a certain limit, the amount of reductive adsorbates (i.e. carboxylate) is not sufficient for the total reduction of γ-Fe_2O_3 to Fe_3O_4 in an inert atmosphere.

In this case the phase transition to α-Fe_2O_3 occurs. If the particle size falls, however, below this limit, the amount of reductive species on the increased surface area becomes sufficient for the reduction to Fe_3O_4 according to the general equation

$$\tfrac{96}{9}(\gamma - Fe_2O_3) + 8x(CO_2^-) \rightarrow {}^{[4]}\left(Fe^{3+}_{\frac{64}{9}}[V]_{(\frac{8}{9}-x)}\right) \times {}^{(6)}\left(Fe^{2+}_{8x}\,Fe^{3+}_{(\frac{128}{9}-8x)}[V]_{(\frac{16}{9}-2x)}\right)O_{32-4x} + 4x(CO_3^{2-}) + 4xCO_2\uparrow \qquad (4)$$

with $0 \leqslant x \leqslant \frac{8}{9}$.

In the case of a complete reduction ($x = \frac{8}{9}$) Equation 4 becomes

$$3Fe_2O_3 + 2\{CO_2^-\} \rightarrow 2Fe_3O_4 + \{CO_3^{2-}\} + CO_2\uparrow \qquad (5)$$

Heating the samples in air leads however to an oxidation of the carboxylate species by oxygen according to Equation 1 at still lower temperature. A more detailed description of these findings is given elsewhere [24].

3.5. Magnetic properties

γ-Fe_2O_3 for magnetic recording is usually prepared by transforming FeOOH via α-Fe_2O_3 and Fe_3O_4 into the final product [25]. The desired H_c values necessary for the recording process are because of the magnetic shape anisotropy of acicular particles. Spherical particles reveal low coercivities corresponding to low anisotropy fields caused by the cubic spinel structure.

Magnetic particles with sizes in the range of about 100 nm (depending on the material) show stable single domain behaviour. A size decrease to below a critical limit leads to significant changes of the magnetic properties called superparamagnetism, e.g. no remanent

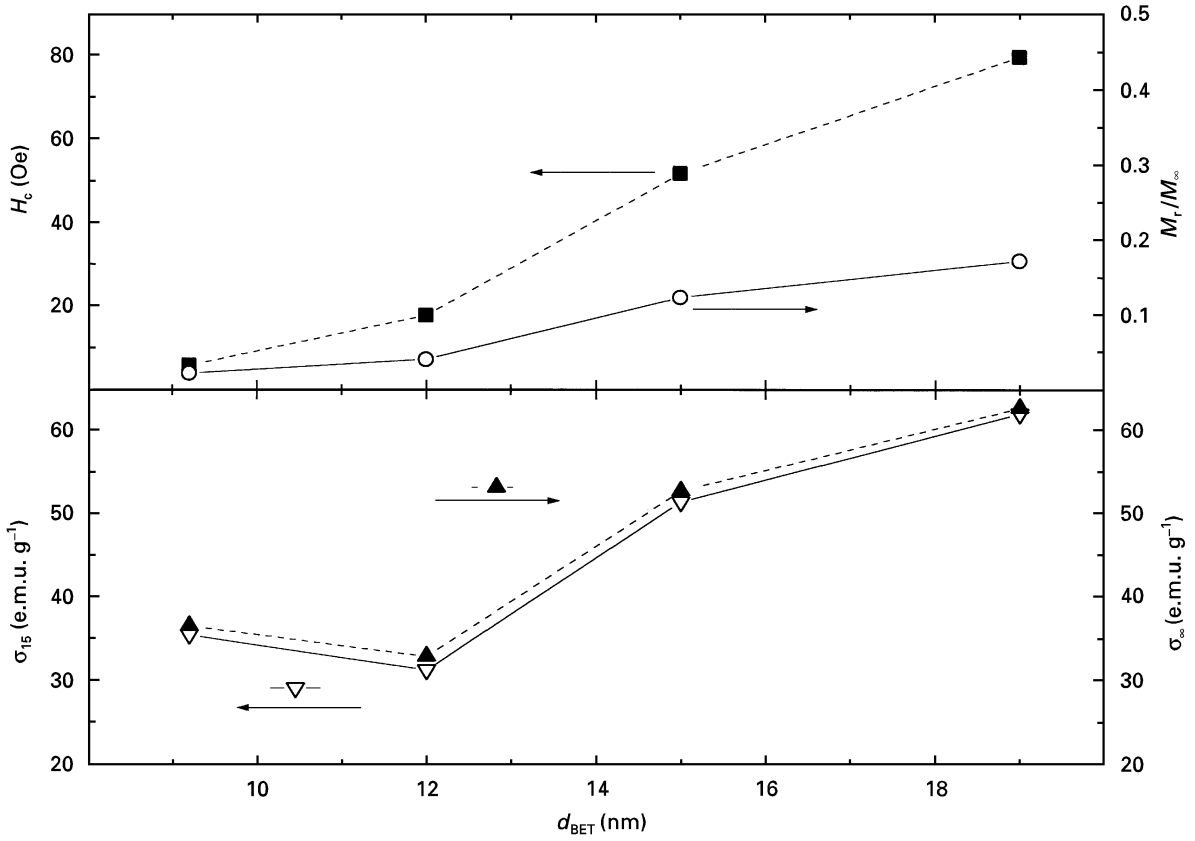

Figure 7 Variation of the magnetic properties in relation to the particle sizes of the ultrafine γ-Fe_2O_3 powders under investigation.

magnetization and no coercivity is observable. The magnetic properties of the γ-Fe_2O_3 powders in relation to particle size are plotted in Fig. 7. The specific saturation magnetization values are lower compared with those of bulk γ-Fe_2O_3 ($\sim$65 e.m.u. g^{-1} [26]). The reason could be the influence of magnetic surface effects, e.g. so-called "magnetic dead layers", well known from manganese ferrite [27] or hexaferrites [28] and/or possibly, the fault of the sample mass caused by adsorbed material as described below.

The decay of the σ_∞-curve at low particle sizes is due to the increasing influence of surface effects corresponding to the S_{BET} values. Apart from the influence of the anisotropy field mentioned above, the low coercivity and remanence values for small particle sizes are probably caused by the contribution of superparamagnetic particles. The mean particle size of all samples is lower than the critical size for the transition to superparamagnetism [29]. In solution, the powders can be deagglomerated down to hydrodynamic diameters of 40 nm obtained from light scattering experiments. The fact, that after more than 24 h the resulting colloidal solution shows visually no indication for sedimentation can be interpreted in terms of weak magnetic interactions between the dispersed particles. Otherwise, the magnetic attraction should cause aggregation and, in consequence, sedimentation.

4. Conclusions

From our investigations it appears that the combustion of iron pentacarbonyl and iron(III)-acetylacetonate, respectively, in an oxyhydrogen flame lead always to γ-Fe_2O_3. Considering this amazing result together with the numerous findings in the literature about the formation of iron oxides through gas phase reactions, described above [4–13], a more complex hypothesis for phase formation under such extreme conditions should be supposed.

1. A strict determination must be made between particle formation by vapour phase condensation and particle formation via decomposition of aerosol droplets. In the latter case the nature of the precursor immediately influences the phase formation, whereas in the former one such a correlation does not exist.
2. Fast condensation of iron oxides from the gaseous state in an intense temperature gradient at first forms the simplest package of anions, i.e. the face centred cubic one, causing the preferred formation of γ-Fe_2O_3, independent of the temperature and the oxidation states of the starting material. This agrees well with similar investigations on aluminas [30] and other oxide powders. A phenomenological description of this behaviour is well known as "Volmers rule" [31].
3. The content of Fe^{2+} in the reaction product is mainly determined because of

(i) the stoichiometric ratio of fuel and oxygen in the flame. In the case of incomplete combustion (excess of fuel) the stability of Fe^{2+} is high enough even to yield magnetite ($Fe^{2+}Fe_2^{3+}O_4$), as described in the BASF patent [14].
(ii) the temperature of the flame.
(iii) the degree of quenching after burning (reoxidation).

4. The formation of α-Fe_2O_3 in the flame is only possible, if the retention time in the temperature range above 460 °C is high enough for the phase transition γ-$Fe_2O_3 \rightarrow \alpha$-$Fe_2O_3$. Since the quenching rate decreases with increasing particle size, the formation of α-Fe_2O_3 only occurs, if the particles exceed a critical size.

Additionally to point 2 the formation of γ-Fe_2O_3 can also be explained on the basis of a structure–chemical/kinetic consideration.

The quite general formula in Equation 4 reflects the strong structural changes which occur during the phase transition from γ-Fe_2O_3 to Fe_3O_4 and vice versa. Although both phases possess the spinel structure, the one of γ-Fe_2O_3 is a defect spinel in which the Fe^{3+} ions together with the resulting vacancies are randomly distributed among the tetrahedral and octahedral sites in the following manner (note, that γ-Fe_2O_3 corresponds to $x = 0$ in Equation 4)

$$^{[4]}\left(\mathrm{Fe}^{3+}_{\frac{64}{9}}[\mathrm{V}]_{\frac{8}{9}}\right)^{[6]}\left(\mathrm{Fe}^{3+}_{\frac{128}{9}}[\mathrm{V}]_{\frac{16}{9}}\right)\mathrm{O}_{32} \qquad (6)$$

The high degree of disorder is the strong clue as to explain why γ-Fe_2O_3 is formed during our experiments, independently of the nature of the starting material. The extremely short retention time in the oxyhydrogen flame together with the extraordinarly high cooling rate after burning does not allow any ordering of the cations among the tetrahedral and octahedral sites of the spinel structure, as is necessary for the formation of Fe_3O_4, which can be described as

$$^{[4]}\left(\mathrm{Fe}^{3+}_{\frac{64}{9}}\right)^{[6]}\left(\mathrm{Fe}^{2+}_{\frac{64}{9}}\mathrm{Fe}^{3+}_{\frac{64}{9}}\right)\mathrm{O}_{28\frac{4}{9}} \qquad (7)$$

Even if Fe^{2+} ions are formed in the oxyhydrogen flame due to extremely high temperatures, these were incorporated into the defect spinel structure and stabilized by adsorbed CO_2 and the described electron transfer according to Equation 1, giving always γ-Fe_2O_3. Therefore in the case of a gas phase reaction the regime of quenching determines first of all the resulting iron oxide phase.

- Intense quenching from high temperature favours the formation of γ-Fe_2O_3.
- increasing retention time above 460 °C prefers the phase transition to α-Fe_2O_3.
- increasing retention time below 460 °C leads in the presence of sufficient Fe^{2+} to Fe_3O_4.

On the basis of this assumption the frequently described occurrence of multiphase iron oxide powder as a result of a combustion process can be easily interpreted in terms of fluctuations in the quenching rate as well as in the flame temperature during pyrolysis and in terms of a broad particle size distribution of the resulting powders, leading to quite different "thermal experiences" of the particles on cooling.

References

1. R. KRIEGEL, J. TÖPFER, N. PREUSS, ST. GRIMM and J. BÖER, *J. Mater. Sci. Lett.* **13** (1994) 1111.
2. S. MUSIC, M. GOTIC, S. POPOVIC and I. CZAKO-NAGY, *Mater. Lett.* **20** (1994) 143.
3. K. SURESH and K. C. PATIL, *J. Mater. Sci. Lett.* **12** (1994) 572.
4. A. KATO and F. TOKUNAGA, *Funtai Oyobi Funmatsu Yakin* **24** (1977) 1.
5. M. KAGAWA, F. HONDA, H. ONODERA and T. NAGAE, *Mater. Res. Bull.* **18** (1983) 1087.
6. T. GONZÁLES-CARREÑO, M. P. MORALES, M. GRACIA and C. J. SERNA, *Mater. Lett.* **18** (1993) 151.
7. M. V. CABANAS, M. VALLET-REGI, M. LABEAU and J. M. GONZALES-CALBET, *J. Mater. Res.* **8** (1993) 2694.
8. M. P. MORALES, C. DE JULIAN, J. M. GONZALES and C. J. SERNA, *ibid.* **9** (1994) 135.
9. E. WEDEKIND and W. ALBRECHT, *Berichte* **70** (1926) 1728.
10. V. KOHLSCHÜTTER and J. W. TÜSCHER, *Z. Elektrochem.* **45** (1921) 225.
11. V. CAGLIOTTI and O. D'AGOSTINO, *Gazz. Chim. Ital.* **66** (1936) 543.
12. R. HAUL and T. SCHOON, *Z. Elektrochem.* **45** (1939) 663.
13. A. WINKEL and R. HAUL, *ibid.* **44** (1938) 823.
14. BASF AG, DT-Patent 830 946 (1949).
15. DEGUSSA DE, 762 723 (1942).
16. G. W. KRIECHEBAUM and P. KLEINSCHMIDT, *Angew. Chem. Adv. Mater.* **101** (1989) 1446.
17. W. HARTMANN, T. A. LIU, D. PEUKERT and P. KLEINSCHMIDT, *Mater. Sci. Engng* **A109** (1989) 243.
18. E. WAGNER and H. BRÜNNER, *Angew. Chem.* **72** (1960) 745.
19. T. GONZÁLES-CARREÑO, M. P. MORALES and C. J. SERNA, *J. Mater. Sci. Lett.* **13** (1994) 381.
20. ST. GRIMM, J. BÖER and S. BARTH, in Proceedings of VII. Vortragstagung Festkörperchemie als Grundlage der Materialwissenschaften, Bonn, 1994.
21. G. L. MESSING, S.-C. ZHANG and G. V. JAYANTHI, *J. Amer. Ceram. Soc.* **76** (1993) 2707.
22. R. SCHRADER and G. BÜTTNER, *Z. Anorg. Allg. Chem.* **320** (1963) 204.
23. M. L. HAIR, "Infrared spectroscopy in surface chemistry" (Marcel Dekker Inc., New York, 1967).
24. ST. GRIMM, J. LEUTHÄUSSER, TH. STELTZNER, S. BARTH and K. HEIDE, *Thermochim. Acta* **300** (1997) in prep.
25. P. KLINGELHÖFER, L. MAROSI and E. SCHWAB, *J. Magn. Mater.* **101** (1991) 248.
26. LANDOLT-BÖRNSTEIN, "Numerical Data and Functional Relationships in Science and Technology", New Series, Group III, Vol. 4a (Editor-in-Chief, K.-H. Hellwege) (Springer-Verlag, 1970) p. 18.
27. Z. X. TANG, C. M. SORENSEN, K. J. KLABUNDE and G. C. HADJIPANAYIS, *J. Appl. Phys.* **69** (1991) 5279.
28. S. KIRUSU, T. IDO, H. YOKOYAMA, *IEEE Trans. Magn.* **23** (1987) 3137.
29. A. BERKOWITZ, W. J. SCHUELE and P. J. FLANDERS, *J. Appl. Phys.* **39** (1968) 1261.
30. S. GRIMM, Dissertation, University of Jena, 1996.
31. M. VOLMER, "Zu Kinetik der Phasenbildung und Elektronenreaktionen" (Akademische Verlagsgesellschaft Geest und Portig, Leipzig, 1984).

Received 30 August 1995
and accepted 3 September 1996